2011 International Symposium on Nonlinear Theory and its Applications
NOLTA2011, Kobe, Japan, September 4-7, 2011

MMO-Adding Phenomena in the Driven Bonhoeffer-van der Pol Oscillator

Yuto Saito†, Kuniyasu Shimizu†, Munehisa Sekikawa‡, Naohiko Inaba¶ and Yutaka Haga†

†Department of Electrical, Electronics and Computer Engineering, Chiba Institute of Technology 275-0016, Japan
‡Institute of Industrial Science, the University of Tokyo 153-8505, Japan
¶Organisation for the Strategic Coordination of Research and Intellectual Property, Meiji University 214-8571, Japan

Email: s1172019QE@it-chiba.ac.jp, kuniyasu.shimizu@it-chiba.ac.jp

Abstract—Mixed-mode oscillations(MMOs) have been a hot topic in recent years. In this paper, we report discovery of MMO-adding phenomena generated by the Bonhoeffer-van der Pol oscillator under weak periodic perturbation. Period-adding is a well-known phenomenon often caused in a MMO-sequence. MMO-adding is a phenomenon where another MMO sequence is added gradually to the base MMO sequence. MMO-adding phenomena are generated successively. As far as numerical results are concerned, these phenomena are often observed between various neighboring successive two MMOs.

1. Introduction

Mixed-mode oscillations (MMOs) are nonlinear phenomena where the solution has complicated waveforms with alternating large- and small-amplitude excursions in the observed time series. MMOs are a subject of intensive research in wide variety fields (*cf.* [1–6], and some references therein). As an example, in the context of neuronal activity, their observation in the Hodgkin-Huxley model [2] are known. In nervous system, it is important to understand a neural excitability. The MMOs is strongly related to bursting activities in neurons.

The Bonhoeffer-van der Pol (BVP) oscillator is an attractive model for understanding behavior of neurons because it is known as a simplified Hodgkin-Huxley model [7–9]. Ravinovich *et al.* pointed out in [8, 9] that the BVP oscillator possesses rich dynamics because a subcritical Andronov-Hopf bifurcation (AHB) can occur. In the vicinity of the subcritical AHB point, a focus and a relaxation oscillation can coexist in close proximity.

We focus on phenomena if weak periodic perturbation is applied to the BVP oscillator when the parameter set is chosen at the neighborhood of the subcritical AHB point. In our previous work, we reported that this dynamics can produce various types of MMOs [6]. Between existence regions of the two neighboring MMOs, chaotic phenomena and periodic steady states can be observed alternately.

In this paper, we pay attention to the periodic steady states which are concerned with the MMOs. We discover various sequence patterns consisting of several sequences of the two neighboring MMOs. Especially, the attractor increases the number of the comprising sequences of MMOs as the parameter corresponding to an angular frequency of the forcing term is changed. We compare the property with that of the MMOs by calculating 1-parameter bifurcation diagram and the largest Lyapunov exponent.

2. Bifurcations in the BVP oscillator

The driven BVP oscillator is expressed by the second order non-autnomous differential equation as follows referring to [6]:

$$\begin{aligned} \varepsilon\dot{x} &= y - (-x + x^3) \\ \dot{y} &= -x - k_1 y + B_0 + B_1 \sin\omega\tau \qquad (\frac{d}{d\tau} = \cdot). \end{aligned} \tag{1}$$

We assume that $\varepsilon \ll 1$, and in this case the dynamics of Eq.(1) is a slow-fast system. We fix $\varepsilon = 0.1$ throughout this study. The other parameters are chosen in terms of the situation described below. In particular, we employ a weak periodic forcing term, namely the case of small B_1 value.

In this section, we investigate the case where no periodic perturbation is applied to this dynamics, namely $B_1 = 0$. If the value of k_1 is zero, the circuit is well-known van der Pol oscillator. In this case, for large B_0, an equilibrium point of Eq.(1) is a stable. When B_0 becomes smaller, the stable focus losses the stability and a limit cycle is born by the supercritical Andronov-Hopf bifurcation (AHB). In other words, the steady state changes at the supercritical Andronov-Hopf bifurcation (AHB) point. The van der Pol oscillator has always only one attractor. Note that the situation for small k_1 is the same as above.

In contrast, for larger k_1, the subcritical AHB can take place. Figure 1 presents 1-parameter bifurcation diagram for $k_1 = 0.9$. In the figure, the abscissa and ordinate denote the parameter B_0 and the value

of x, respectively. This figure is obtained using XPPAUT [10]. The solid and dotted lines denote a stable and an unstable focus, respectively. The filled circles present the extrema of a relaxation oscillation. The open circles show the extrema of an unstable periodic oscillation. In this case, the subcritical AHB occurs at the point $B_0^c(\approx 0.20543)$. It should be noted that the following three cases appear according to the value of B_0. (a) $B_0 > B_0^f(\approx 0.211)$, there exists a stable focus only. (b) $B_0^c \leqq B_0 \leqq B_0^f$, a stable focus, an unstable limit cycle, and a relaxation oscillation coexist. (c) $B_0 < B_0^c$, a relaxation oscillation is observed as a steady state. In the cases of (a) and (c), the dynamics has only one stable attractor. On the other hand, in the case of (b), either the stable focus or the relaxation oscillation appears depending on the initial state. In this paper, we pay attention to the latter situation, because from the Fig.1, two stable solutions coexist in close proximity. Then, we are interested in how the dynamics is influenced when weak periodic perturbation is applied to the circuit in the case of (b). In the following discussions, we fix the parameters $k_1 = 0.9$, $B_0 = 0.207$, and we apply weak periodic perturbation ($B_1 = 0.01$) to this dynamics[1].

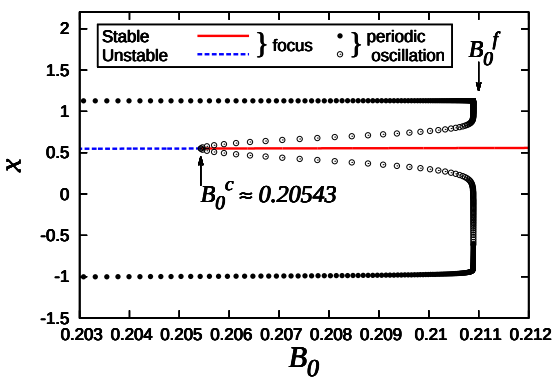

Figure 1: Structure in the vicinity of the subcritical AHB point for $k_1 = 0.9$.

3. MMO-adding phenomena

In our previous work, we reported the discovery of the sequences of MMOs from the BVP oscillator under weak periodic perturbation [6]. First, we review these MMOs.

Figure 2 shows an example of MMOs for $\omega = 0.57$, where time series plots of x, and the trajectory on the phase plane with the nullclines of Eq.(1) and a

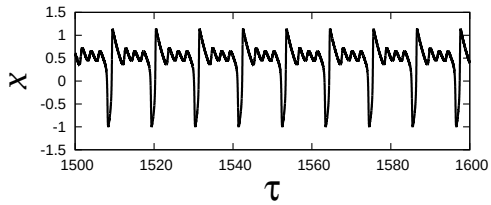

(a) Time series plot.

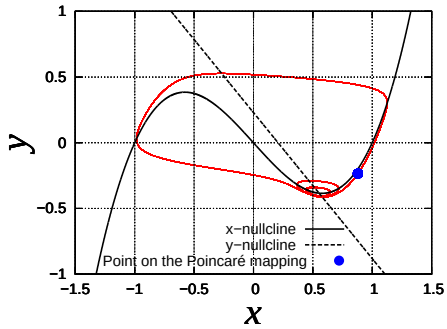

(b) Trajectory on the phase plane.

Figure 2: Example of MMOs for $\omega = 0.57$ (1^3).

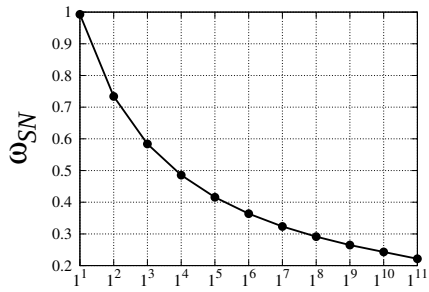

Figure 3: Saddle-node bifurcation point (ω_{SN}) of the 1^s ($1 \leqq s \leqq 11$).

point on the Poincaré mapping[2] are presented. The sequence consists of one large excursion and three small peaks in one period. Note that the trajectory clearly moves back and forth periodically between the stable focus and the relaxation oscillation. To distinguish various sequences of MMOs, we introduce the notation L^s referring to [1], where L denotes the number of large-amplitude excursions, and s represents that of small-amplitude peaks.

By decreasing ω, we find the sequences 1^s where the number of small peaks s increases monotonically. So far, for $0 < \omega < 1$, we find that s changes from 1 to 11 with the appropriate values of ω. A saddle-node(SN) and a period-doubling(PD) bifurcation occur at ω_{SN} and ω_{PD}, respectively. By decreasing ω, the sequence 1^s appears at ω_{SN}, and disappears at ω_{PD}. The values of ω_{SN} and ω_{PD} are calculated by the method

[1] All numerical integrations of Eq.(1) are conducted by fourth-order Runge-Kutta method with a step size $2\pi/\omega/1024$, and we set the initial state $(x_0,\ y_0)$ to $(0, 0)$ throughout this paper.

[2] We take the Poincaré mapping at every $\tau = 2\pi n/\omega$, where n is an integer.

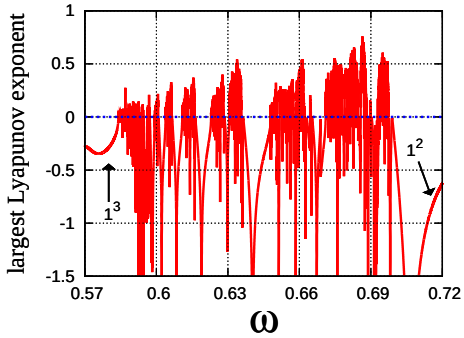

Figure 4: Variation of largest Lyapunov exponent for $0.57 \leqq \omega \leqq 0.72$.

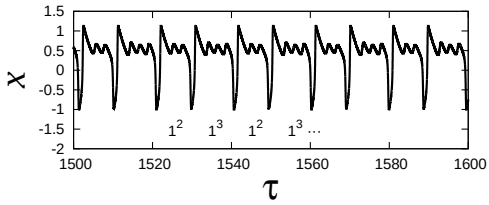

(a) Time series plot.

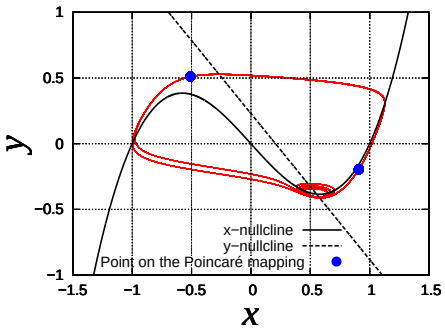

(b) Trajectory on the phase plane.

Figure 5: Alternation of sequences between the 1^2 and 1^3 for $\omega = 0.64$ ($[1^2, 1^3 \times 1]$).

proposed by Kawakami [11]. Figure 3 shows the values of ω_{SN} of the 1^s. From the figure, the ω_{SN} decays exponentially as s increases.

Next, we explain what behavior is observed between the existence regions of 1^s and 1^{s+1}. Figure 4 shows the graph of the largest Lyapunov exponent between the existence regions of 1^2 and 1^3. The exponent is calculated by the algorithm of Shimada and Nagashima [12]. Both existence regions of 1^2 and 1^3 are indicated by their labels with the arrowed lines. As far as numerical result is concerned, it is suggested that crucial complicated phenomena and its related bifurcations can occur. In particular, chaotic phenomena and periodic steady states can be observed alternately when the value of ω is gradually changed. In the following, we focus on the periodic steady states which are concerned with the sequences of MMOs.

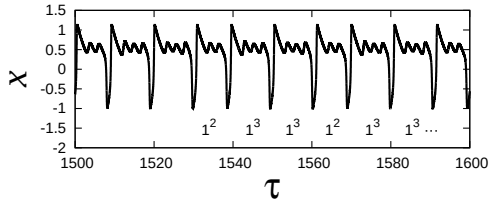

Figure 6: The sequence pattern consisting of the 1^2 and the two series of 1^3 for $\omega = 0.62$ ($[1^2, 1^3 \times 2]$).

Table 1: Values of ω_{SN} and ω_{PD} of the solution $[1^2, 1^3 \times n]$ and its period of the Poincaré mapping.

n	Solution	ω_{PD}	ω_{SN}	Period
1	$[1^2, 1^3 \times 1]$	0.63643	0.64803	2
2	$[1^2, 1^3 \times 2]$	0.61633	0.62294	3
3	$[1^2, 1^3 \times 3]$	0.60658	0.61085	4
4	$[1^2, 1^3 \times 4]$	0.60090	0.60385	5
5	$[1^2, 1^3 \times 5]$	0.59723	0.59937	6
6	$[1^2, 1^3 \times 6]$	0.59470	0.59630	7
7	$[1^2, 1^3 \times 7]$	0.59287	0.59409	8
8	$[1^2, 1^3 \times 8]$	0.59149	0.59245	9
9	$[1^2, 1^3 \times 9]$	0.59042	0.59118	10
10	$[1^2, 1^3 \times 10]$	0.58957	0.59019	11
11	$[1^2, 1^3 \times 11]$	0.58889	0.58940	12
12	$[1^2, 1^3 \times 12]$	0.58865	0.58875	13
13	$[1^2, 1^3 \times 13]$	0.58815	0.58822	14

Figure 5 shows a periodic steady state with interesting property. From Fig.5(a), the waveform follows such a pattern that the sequences of 1^2 and 1^3 appear alternately. The sequence pattern is periodic solution with period 2 and this sequence is denoted by $1^2 1^3$. For slightly smaller ω, there exists another periodic sequence pattern. Figure 6 displays the discovered possible pattern which consists of the sequence of 1^2 and two series of 1^3. In this case, the attractor is the periodic solution with period 3 and the sequence pattern should be denoted by $1^2 1^3 1^3$. This phenomenon should be called *MMO-adding phenomenon*. Remark that the this phenomenon occurs successively.

To define the sequence generated by MMO-adding phenomena the notation 1^s is extended to $[1^s, 1^{s+1} \times n]$, where n denotes the number of the series of 1^{s+1} sequences. From a numerical calculation, the sequence pattern $[1^s, 1^{s+1} \times n]$ corresponds to a $(n+1)$ periodic point of the Poincaré mapping. The PD and the SN

bifurcation occur at ω_{SN} and ω_{PD}, respectively, which is quite same in the case of MMOs. Table 1 presents the values of ω_{SN} and ω_{PD} of the solution $[1^2, 1^3 \times n]$ $(n = 1, 2, \cdots, 13)$ and its period of the Poincaré mapping. Figure 7 shows $\Delta\omega$ of the $[1^2, 1^3 \times n]$. The ω_{SN} of the $[1^2, 1^3 \times n]$ becomes smaller for larger n. Compared to Fig.3, both shapes of graph resemble each other although the scale of vertical axis is not same.

Figure 8 displays a 1-parameter bifurcation diagram[3] with respect to ω and the corresponding largest Lyapunov exponent. The axis range of abscissa is chosen around the existence region of 1^3. When ω is decreased from 0.6, a multiple periodic solution $[1^2, 1^3 \times n]$ changes to chaos via succeeding PD bifurcations, and then settles down to the neighboring periodic state, namely $[1^2, 1^3 \times n + 1]$. Such phenomenon continues many times. In other words, the cascade structure can be observed as shown in Fig.8 which should be investigated more in detail.

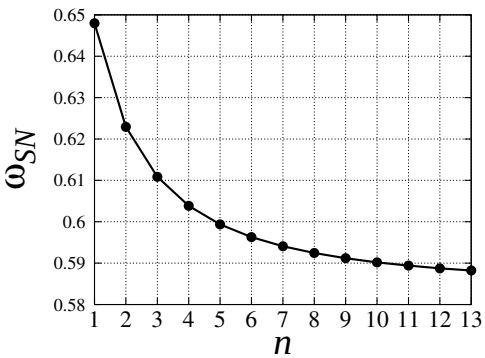

Figure 7: Saddle-node bifurcation point (ω_{SN}) of the $[1^2, 1^3 \times n]$.

4. Concluding remarks

We reported that the complicated behaviors can be produced from the simple driven oscillator where periodic perturbation is small. In particular, we discovered the MMO-adding phenomena observed between the existence regions of the two neighboring MMOs. Since the complicated sequence patterns including the MMOs are periodic steady states, we will investigate the phenomena more in detail from the dynamical point of view in the nearest future.

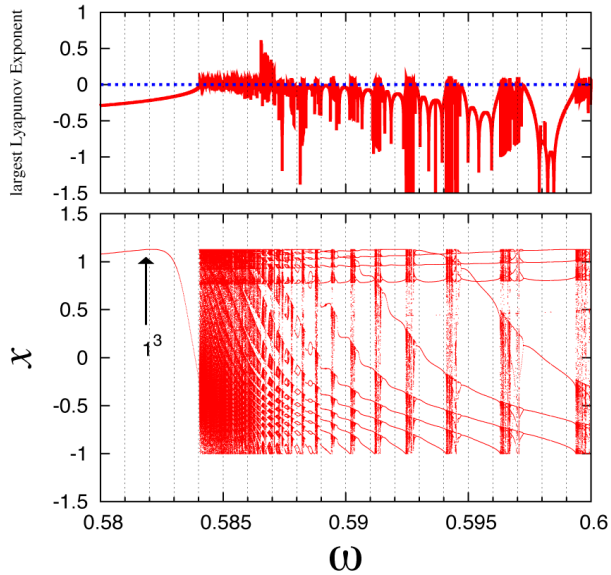

Figure 8: 1-parameter bifurcation diagram and the corresponding largest Lyapunov exponent for $0.58 \leqq \omega \leqq 0.60$.

References

[1] A. Milik, P. Szmolyan, H. Löffelmann, E. Gröller, Int. J. Bifurc. Chaos 8 (1998) 505.

[2] J.Rubin and M.Wechselberger, Biol,Cybern., 97, 1 (2007) 5.

[3] G.Medvedev and Y.Yoo, Chaos 18 (2008) 033105.

[4] K.Klomkarn and P.Sooraksa, Int. J. Bifurc. Chaos 20 (2010) 1485.

[5] M.Sekikawa, N.Inaba, T.Yoshinaga and T. Hikihara, Phys. Lett. A, 374, (2010) 3745.

[6] K.Shimizu, M.Sekikawa and N.Inaba, Phys. Lett. A, 375, (2011) 1566.

[7] S. Sato and S. Doi, Math. Biosci. 112 (1992) 243.

[8] A.Rabinovitch, R.Thieberger, M. Friedman and S. Goshen, Chaos, Solitons & Fractals 7 (1996) 1713.

[9] A.Rabinovitch and I.Rogachevskii Chaos 9 (1999) 880.

[10] B.Ermentrout, Simulating, analyzing, and animating dynamical systems: A guide to XPPAUT for researchers and students, SIAM, Philadelphia, (2002).

[11] H.Kawakami, IEEE Trans.Circuits.Syst., 31, 3 (1984) 248.

[12] I.Shimada and T.Nagashima, Prog. Thor. Phys., (1979) 1605.

[3] The points on the Poincaré mapping of x at $\tau = 2\pi n/\omega$ $(500 \leqq n \leqq 1000)$ are plotted for each ω.